The 2020 World Congress on
Advances in Civil, Environmental, & Materials Research (ACEM20)
25-28, August, 2020, GECE, Seoul, Korea

Progressive search method for determining basal heave failure surface of excavation in anisotropic clay

Hong Li[1)], Liu Han-Long[2)], *Zhang Wen-gang[3)]

[1), 2),3)] *Department of Civil Engineering, Chongqing University, Chongqing 400045, China*
[3)]*Cheungwg@126.com*

ABSTRACT

Determining the failure surface is a key point in basal stability analysis of braced excavations in soft clay. In general, for limit equilibrium (LEM) and upper bound analysis method, the failure surfaces are assumed. In this study, progressive search method was proposed. It includes three parts. Firstly, random number method was adopted to generate several initial failure surfaces. Secondly, multi-block upper bound method was adopted to establish power equation and calculate the safety factor of each failure surface. Thirdly, from the initial failure surfaces to the critical failure surfaces, an algorithm of search is necessary. So, the progressive search algorithm was adopted. In order to describe the behavior of anisotropic soil, the anisotropic criterion was applied to multi-block method. Based on the examples and case study, suggestions with regard to the number of initial surfaces, the number of searches were proposed. Compared with the shear strength reduction in finite element method (SSR-FEM), it is verified that progressive search method is reasonably used to basal stability analysis of braced excavation in anisotropic clay.

Key words: basal stability analysis, braced excavations, anisotropic soil, multi-block upper bound method, progressive search algorithm.

1. INTRODUCTION

Basal stability analysis plays an important role in braced excavation in soft soils. Recently, the methods of basal stability analysis mainly include limit equilibrium method (LEM) (Goh 1994,2008), shear strength reduction in finite element method (SSR-FEM) and upper bound method (Afiri 2017, Faheem 2003, Goh 2017a, 2017b). Upper bound method was proposed by Drucker (1952) and was firstly applied to structure engineering. Based on the characteristics of soil and rock materials, Chen et al. applied upper bound method to bearing capacity analysis of foundations and stability analysis of slopes (Chang 2000, Chen 1975, Chen 2015, Gao 2015, Han 2014, Huang 2009, 2018, Michalowski, 2009). Based on the previous work, upper bound methods include upper bound finite element method (Ukritchon 2003), multi-block method (Huang 2009, Qin 2010b) and traditional analytic upper bound method (Chang 2000, Huang 2018, Cai 2018). Compared to upper bound finite element method and other upper bound methods, multi-block method requires fewer assumptions and is easy for realization.

---

1) Professor
2) Postgraduate
3) Professor

For braced excavation in soft soils, LEM and SSR-FEM were universally applied to analyze basal stability. However, the use of multi-block method in braced excavation was less reported. In this paper, multi-block method was adopted for braced excavation. In addition, the progressive search method was adopted to optimize the determination of the failure surfaces; and the anisotropic strength criterion was adopted to describe the behavior of the soft anisotropic soils.

Currently, for anisotropic soils, anisotropic constitutive model (Mroz 1978, 1979), random finite element analysis (REFM) (Luo 2020, Chen 2019) and anisotropic strength criteria are general methods. Based on the anisotropic constitutive model, it is possible for us to propose related design methods or carry out integrated numerical simulations. However, the shortcoming is the material parameters for anisotropic constitutive model are difficult to determine. For example, the NGI-ADP model in PLAXIS is an anisotropic model which needs 10 parameters of strength and stiffness in 2D, while the Mohr-Coulomb model just needs 5 parameters. In addition, the anisotropic tests for soils are expensive than general tests. For RFEM, its core idea is that generate a finite element model with soil strength and stiffness following spatial variability based on the statistical characteristics of soil strength and stiffness. For anisotropic strength criterion of soil, it was first proposed by Casagrande (1944), which assumed that the soil shear strength was related with the direction of failure surfaces. Currently, the anisotropic criteria are widely applied to geotechnical engineering, especially in stability analysis (Su 1998, Wang 2014). Based on the advantages and disadvantages of each method, the second method and third method are applied widely. The third method was adopted to describe the behavior of anisotropic soil.

2. Multi-Block upper bound method

2.1 Basic theory

There are many expressions for limit analysis. In this paper, the following power equation is adopted. Eq. (1) means energy dissipation power is not less than external power for all kinematically admissible velocity fields.

$$\int_S T_i\, v_i dS + \int_V X_i v_i dV \le \int_V \sigma_{ij}\dot{\varepsilon}_{ij}\, dV \quad i,j = 1,2,3 \tag{1}$$

where $\dot{\varepsilon}_{ij}$ is the plastic strain rate in the admissible velocity field; v_i is the velocity field (compatible velocity field) which is geometrically compatible with $\dot{\varepsilon}_{ij}$; X_i and T_i are the surface force on boundary *S* and the volume force in space *V*, respectively; σ_{ij} is the stress which is satisfied the associated flow rule. For any kinematically admissible failure

The calculation processes of upper bound method include four part: firstly, establishing kinematically admissible failure mechanism; secondly, calculating the velocity field which satisfies compatible conditions; thirdly, establishing the power equation; lastly, calculating safety factors.

2.2 Kinematically admissible failure mechanism

According to the previous study of upper bound analysis (Huang 2018, Qin 2010a, 2010b, 2012), the failure surfaces of basal heave in excavation are usually circle slip plane (Fig. 1).

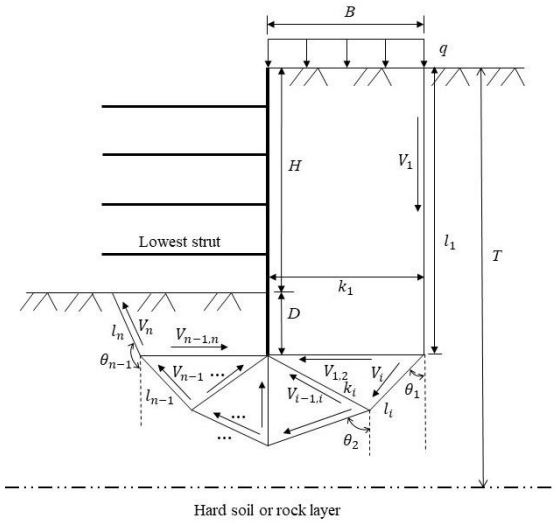

Fig. 1 Kinematically admissible failure mechanism of upper bound analysis

In Fig. 1, the support system was assumed rigid so that the failure surfaces would not cross diaphragm wall. Similarly, it is assumed that the failure surfaces would be above the hard soil layer. From Fig. 1, the failure surfaces consisted of n+1 points and n blocks (included two quadrilateral blocks and *n-2* triangle blocks). In order to satisfy accuracy of calculation, enough triangle blocks were needed. And in the section 3.3, this problem would be discussed. Other notations were showed in Table 1.

Table 1 Explanations of Symbols

Symbol	Description
B/m	Width of excavation
H/m	Depth of excavation
D/m	length of support wall below the finial excavation surface
T/m	Depth of hard soil or rock layer
k_i/m	Length of interface between two adjacent blocks
l_i/m	Length of failure surface of each block
$\boldsymbol{v_i}$	Speed vector in the surface of l_i
$\boldsymbol{v_{i,i+1}}$	Speed vector in the surface of k_i
θ_i	Angle between $\boldsymbol{v_{i+1}}$ and negative vertical direction (assuming down is negative)

Based on compatible conditions of kinematical field, $\boldsymbol{v_i}$ and $\boldsymbol{v_{i,i+1}}$ can be calculated by Eq. (2):

$$\boldsymbol{v_{i+1}} = \boldsymbol{v_i} + \boldsymbol{v_{i,i+1}} \quad i = 1,2,\cdots,n-1 \tag{2}$$

From Eq. (2), if directions of three vectors and value of one vector are known, all values can be calculated. In this paper, all directions of vectors are obtained from failure surfaces, and it is assumed that $\boldsymbol{v_1}$ equals to 1. The detailed derivation is provided in reference (Qin 2012, Zou 2004).

2.3 Application to basal stability analysis of excavation in anisotropic soils

In Eq. (1), the power equation includes external power and energy dissipation power. For basal stability analysis of excavation, the external power includes soil

gravity and upper load; the energy dissipation power includes dissipation at interfaces between adjacent blocks, dissipation at interface between support wall and soil, and dissipation at failure surfaces (Eq. (3)).

$$\sum_{i=1}^{n} w_i v_i cos\theta_i + q v_1 k_1 \leq \sum_{i=1}^{n} S_u l_i v_i + \sum_{i=1}^{n-1} S_u k_i v_{i,i+1} + \omega S_u v_1 l_1 \quad (3)$$

Where q is upper load, S_u is the undrained shear strength, w_i is the weight of each block, ω is the reduction factor, ranges from 0 to 1, which is related with the stiffness of support system.

Eq. (3) was applied to homogeneous and isotropic soils. Generally, the soils are inhomogeneous and anisotropic due to the stress path, pre-consolidation pressure and other reasons. For inhomogeneous soils, it is assumed that the undrained shear strength increases with the depth (Ukritchon 2017, Cheng 2019), which can be expressed as follow:

$$S_{uv}(z) = S_{u0} + \lambda z \quad (4)$$

Where S_{u0} is the undrained shear strength at the ground surface, λ is the rate of shear strength increase with depth, for soft clay λ usually ranges from 1 to 2.

Based on the anisotropic strength theory was proposed by Casagrande et al. (Eq. (5)) (Casagrande 1944), it is assumed that undrained shear strength is related with the angle between the direction of major principal stress and vertical direction. And Ying et al. proposed a modified anisotropic strength theory based on the tests of hollow cylinder apparatus (Eq. (6)) (Chang 1999, Ying 2016).

$$S_u(\xi) = S_{uh}[1 + (k-1)\cos^2 \xi\,] \quad (5)$$

$$S_u(\xi) = S_{uv} \cdot \left[\frac{1+k}{2} + (1-k)\cos\left(2\xi + \frac{\pi}{3}\right)\right] \quad (6)$$

Where ξ is the angle between the direction of major principal stress and vertical direction (the detail calculation of ξ is showed in Fig. 2a and Fig. 2b), k is the factor of anisotropy (usually range from 0.5 to 1.33), which equals to S_{uv}/S_{uh}. S_{uv} and S_{uh} can be obtained from CK_0UC test and CK_0UE test, respectively.

By combining Eq. (5) and Eq. (6), the anisotropic and nonhomogeneous undrained shear strength of soil can be expressed as follow:

$$S_u(\xi, z) = (S_{u0} + \lambda_0 z) \cdot \left[S_{uh}[1 + (k-1)\cos^2 \xi\,]\right] \quad (7)$$

$$S_u(\xi, z) = (S_{u0} + \lambda_0 z) \cdot \left[\frac{1+k}{2} + (1-k)\cos\left(2\xi + \frac{\pi}{3}\right)\right] \quad (8)$$

Eq. (7) was based on the theory proposed by Casagrande (1944), and Eq. (8) was based on the theory proposed by Shen (2006). In this study, Eq. (8) was adopted to describe the behavior of anisotropic soil.

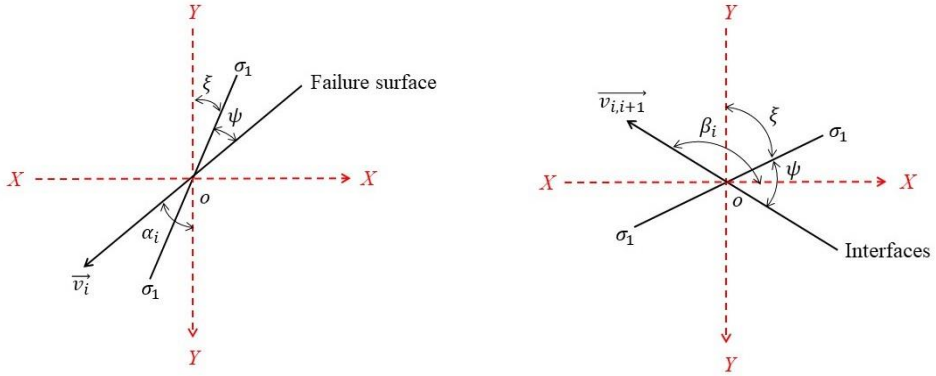

Fig. 2 Calculation of ξ (a) at the failure surfaces, (b) at the interfaces

As shown in Fig. 2, firstly, it is defined that the right of *X* axial is positive and the below of *Y* axial is positive. And the positive direction of failure surface is the same as the vector v_i. α_i is the angle between positive direction of failure surface of i^{th} block and positive direction of *Y* axial. β_i is angle between positive direction of interface of i^{th} block and positive direction of *X* axial. ψ is the angle between failure surface and first principle stress plane (acute angle), based on Mohr-coulomb yielding criteria, $\psi = 45° - \varphi'/2$. ξ is the angle between first principle stress plane and *Y* axial (acute angle). Following above definitions, ξ can be obtained by Eq. (9) and Eq. (10)

$$\xi = \begin{cases} |\alpha_i - \psi|, & \alpha_i \le \frac{\pi}{2} \\ \pi - \alpha_i + \psi, & \frac{\pi}{2} < \alpha_i \le \pi \end{cases} \tag{9}$$

$$\xi = \begin{cases} \left|\frac{\pi}{2} - \beta_i - \psi\right|, & 0 < \beta_i \le \frac{\pi}{2} \\ |\pi - \beta_i + \psi|, & \frac{\pi}{2} < \beta_i \le \pi \end{cases} \tag{10}$$

Note: when α_i or β_i is obtuse angle, ξ calculated by Eq. (9) and Eq. (10) may be obtuse angle, we should adopt its supplementary angle.

In this study, Eq. (8) was adopted to analysis the basal stability of braced excavation. For anisotropic and inhomogeneous soils, Eq. (3) is not suitable. In Fig. 3, an example, calculation of one block, was carried out to explain how to analysis basal stability of excavation in anisotropic and inhomogeneous soils by using multi-block upper bound method.

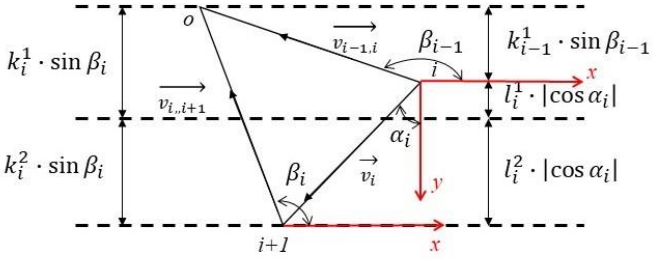

Fig. 3 calculation of one block in multi soil layers

As shown in Fig. 3, it is a bock in two soil layers, we should calculate its dissipation power and external power in first layer and second layer, respectively. For example, the dissipation power at failure surface *i-i+1* (E_i) can be calculated by Eq. (11):

$$\begin{aligned} E_i = &\int_0^{l_i^1} v_i \left[\frac{1+k_1}{2} + (1-k_1)\cos\left(2\xi_i + \frac{\pi}{3}\right)\right] \cdot (S_{u1} + \lambda_1 l|\cos\alpha_i|)dl \\ &+ \int_0^{l_i^2} v_i \left[\frac{1+k_2}{2} + (1-k_2)\cos\left(2\xi_i + \frac{\pi}{3}\right)\right] \cdot (S_{u2} + \lambda_2 l|\cos\alpha_i|)dl \end{aligned} \tag{11}$$

Where l_i^j is the length of i^{th} block in j^{th} soil layer, S_{uj}, λ_j, k_j is the factor of strength in j^{th} soil layer, the definition of α_i is shown in Eq. (9).

Similarly, the dissipation at interface *o-i+1* (F_i) can be calculated. Because the undrained shear strength linearly increases with depth, the integral in Eq. (11) can be simplified by calculating the undrained shear strength at midpoint:

$$E_i = v_i \cdot S_u\left(\xi_i, \frac{l_i^1}{2}\right) \cdot l_i^1 + v_i \cdot S_u\left(\xi_i, \frac{l_i^2}{2}\right) \cdot l_i^2 \tag{12}$$

By combining Eq. (3), Eq. (8) ~ Eq. (12), the total dissipation power (E_d) can be calculated by Eq. (13):

$$E_d = \sum_{i=1}^{n}\sum_{j=1}^{m} l_i^j \cdot v_i \cdot S_u\left(\xi_i, \frac{l_i^j}{2}\right) + \sum_{i=1}^{n-1}\sum_{j=1}^{m} k_i^j \cdot v_{i,i+1} \cdot S_u\left(\xi_i, \frac{k_i^j}{2}\right) + \omega \cdot \sum_{j=1}^{m} l_1^j \cdot S_{uv}\left(\frac{l_1^j}{2}\right) \quad (13)$$

From Eq. (13), E_d includes three parts (dissipation at failure surfaces, dissipation at interfaces between adjacent blocks and dissipation at interface between wall and soils). For the third part, only influence of depth on strength is considered.

The total external power (E_e) can be calculated by Eq. (14):

$$E_e = \sum_{i=1}^{n} w_i v_i \cos\theta_i + q v_1 k_1 \quad (14)$$

In order to satisfy kinematically admissible failure mechanism, the dissipation power should large than external power. Therefore, the safety factor can be defined as follow:

$$F_s = E_d / E_e \quad (15)$$

The safety factor in Eq. (15) and the safety factor in SSR-FEM has a same meaning, which means the margin of shear strength.

3. Progressive search algorithm

In traditional LEM and upper bound method, the failure surfaces are obtained from the assumption. In general, the ratio of excavation width and depth, the friction angle and the coefficient of anisotropy have a great influence on failure surfaces. Progressive search method was proposed by Greco (1996) and Otha (1985), firstly applied to stability analysis of slopes (Malkawi 2001a, 2001b). And Qin et al. adopted it to stability analysis of soil foundations (Qin 2010b). In this paper, progressive search algorithm is adopted to evaluate failure surfaces instead of assuming failure surfaces. Progressive search algorithm includes two parts: firstly, randomly generating initial failures surfaces; secondly, updating failure surfaces by iteration, gradually obtaining critical failure surfaces.

Compared with algorithm proposed by Greco, the algorithm in this paper have two innovations: firstly, adopting new equations to generate initial failure surfaces; secondly, assuming the failure surfaces will not cross support systems (because the support system is assumed rigid) and hard soil layer.

3.1 Generation of initial failure surfaces

The initial failure surfaces include seven points. According to the suggestions of Greco (1996) and Qin (2010b), in order to improve efficiency of calculation, the failure surfaces should concave up. The concave initial failure surfaces can be obtained by followings:

$$\begin{cases} x_1 = (0.5 + 0.5R_1) \cdot B \\ y_1 = 0 \end{cases} \quad (16)$$

$$\begin{cases} x_2 = x_1 \\ y_2 = H + D \end{cases} \quad (17)$$

$$\begin{cases} x_4 = 0 \\ y_4 = H + D + x_1 \end{cases} \quad (18)$$

$$\begin{cases} x_3 = \frac{x_2}{2} \\ y_3 = \left(\frac{y_2 + y_4}{2} + R_2 \cdot \frac{y_4 - y_2}{4}\right) \end{cases} \quad (19)$$

$$\begin{cases} x_6 = -x_1 \\ y_6 = H + D \end{cases} \tag{20}$$

$$\begin{cases} x_5 = \frac{x_6}{2} \\ y_5 = \frac{y_4+y_6}{2} + R_3 \cdot \frac{|y_4-y_6|}{4} \end{cases} \tag{21}$$

$$\begin{cases} x_7 = x_6 - (x_7 - x_6) \cdot |\tan(\alpha_7)| \\ y_7 = H \end{cases} \tag{22}$$

Notes: when $y_5 > T$, should set $y_5 = T$, because the failure surfaces should not cross hard layer. Similarly, when $x_7 < -B$, should set $x_7 = -B$, because the failure surfaces should not cross support wall on the other side.

Where R_1, R_2, R_3 is random number, range from 0 to 1; x_i, y_i is the coordinate of each point; B, H, D are the same as Table 1.

From Eq. (16) to Eq. (22), initial failure surfaces can be obtained. Generally, if only one initial surface is applied to evaluate critical failure surface, a local optimal result may be obtained. Therefore, more initial surfaces are needed to evaluate critical failure surfaces.

3.2 Flowchart of algorithm

After generating initial surfaces, next step is iteration, which is also called process of surfaces search. Search algorithm is shown in Fig. 4.

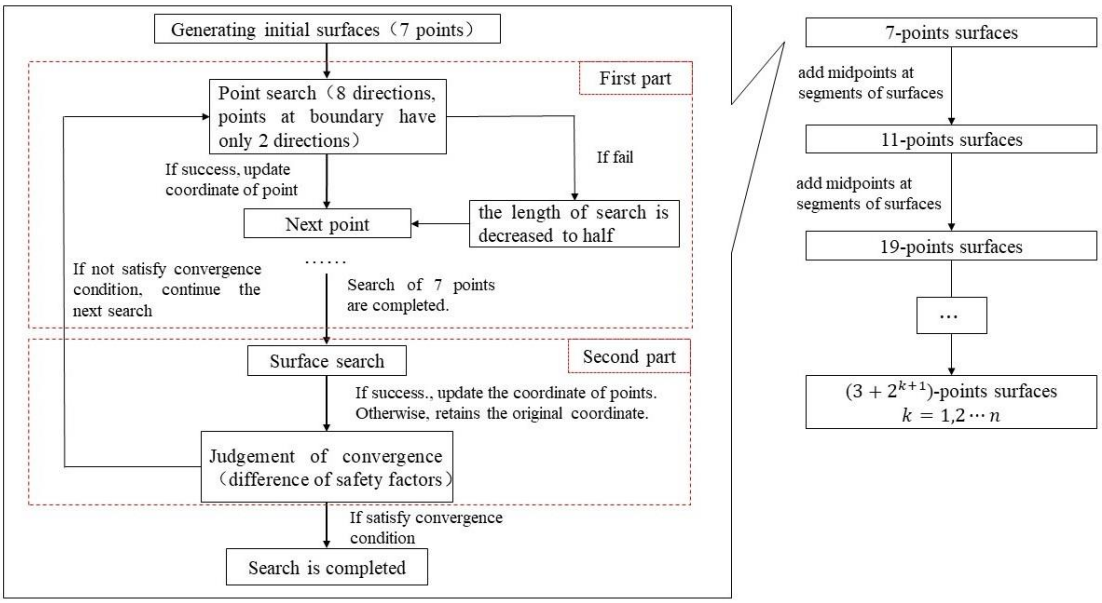

Fig. 4 Flowchart of progressive search method

As shown in Fig. 4, search process includes two parts: search of each point and search of total surfaces. In first parts, each point has eight search directions, some points at boundary have two directions. Eight directions are north, south, east, west and other four directions of diagonals. After all points completed once search, as long as one direction searches successfully (the safety factor after searching is smaller than safety factor before searching), other direction automatically stops search, at the same time, the coordinate of point will be updated. If search of eight directions are failed, the length of search will decrease to half. After all points complete search, second part is search of surfaces. The update of coordinate obeyed followings:

$$\begin{bmatrix} x_i \\ y_i \end{bmatrix}^{k+1} = \begin{bmatrix} x_i \\ y_i \end{bmatrix}^{k} + \boldsymbol{N}\mu_i^k \quad i = 1,2 \cdots n \tag{23}$$

$$\begin{bmatrix} x_i \\ y_i \end{bmatrix}^{e} = 2\begin{bmatrix} x_i \\ y_i \end{bmatrix}^{k+1} - \begin{bmatrix} x_i \\ y_i \end{bmatrix}^{k} \quad i = 1,2 \cdots n \tag{24}$$

Where x_i^k, y_i^k are the coordinate of i^{th} point after *k* times search, ***N*** are the vector controlling search direction, μ_i^k is the length of search of each point after *k* times search, x_i^e, y_i^e are the coordinate of i^{th} point during second part.

Eq. (23) was applied to first part and Eq. (24) was applied to second part. In Eq. (23), ***N*** have 9 kinds of value, which presents 9 kinds of search direction. 9 kinds of value are $(0,0)^T$, $(1,0)^T$, $(0,1)^T$, $(-1,0)^T$, $(0,-1)^T$, $(1,1)^T$, $(1,-1)^T$, $(-1,1)^T$, $(-1,-1)^T$, respectively. Besides $(0,0)^T$, other 8 groups of vector represent 8 kinds of search direction, respectively. Via Eq. (23) and Eq. (24), the integrated search was completed.

Similarly, only the safety factor after searching is smaller than the safety factor before searching, the coordinate would be updated.

Fig. 4 shows an integrated search process of seven-point surfaces. Because number of points at surfaces have a great influence on the accuracy of iteration, more points are needed. New points can be generated by insert midpoint in adjacent points.

3.3 Effect of algorithm application to search failure surfaces

In order to verify the accuracy of algorithm, an example was carried out. The values of parameters are shown in Table 2.

Table 2 The values of parameters

Symbol	Description	Values
B/m	Width of excavation	20
H/m	Depth of excavation	10
D/m	Length of support wall below the finial excavation surface	5
$\gamma/kN \cdot m^{-3}$	Unit weight of soil	19
S_u/kPa	Undrained shear strength	35+2*z*
q/kPa	Upper loading	15
φ'	Effective friction angle	30°
ω	Reduction factor	1

Notes: z is the depth of soils.

Firstly, Eq. (16) ~ Eq. (22) was adopted to generate 50 initial surfaces. The initial surfaces were shown in Fig. 5a. The initial length of search was B/1000, and four phrases of search were adopted to evaluate the critical surfaces. The four phrases are 7 points, 11 points, 19 points, 35 points. The iterations of safety factors are shown in Fig. 5b and the failure surfaces of each phrase are shown in Fig. 5c.

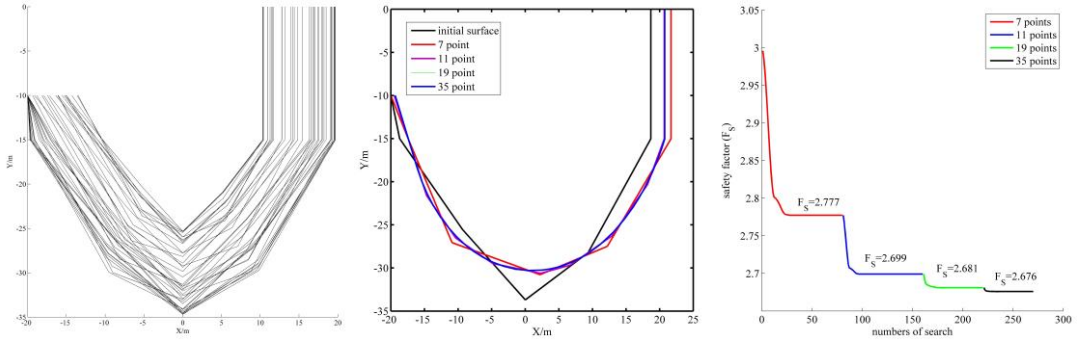

Fig. 5 initial surfaces (a), optimizations of failure surfaces (b) determination of safety factor (c)

From Fig. 5b, it is obvious that the safety factor gradually convergences with the number of searches increasing. If there are mistakes in iterations, this figure will show an abnormal fluctuation. Therefore, it is convenient to verify the accuracy of iteration by checking Fig. 5b. As shown in Fig. 5c, the number of searches of each phrase is 80, 80, 60, 50, respectively. And the safety factor of each phrase is 2.777, 2.699, 2.681, 2.676, respectively. Especially for third phrase and fourth phrase, the failure surfaces almost coincide and the difference of safety factor is only 0.005. In a word, for general basal stability analysis of braced excavation, it is suggested that adopting three phrases to search failure surfaces, and the number of searches of each phrase is 80, 80, 60.

3.4 Comparison with the strength reduction in FEM method

In this section, the example in 3.3 would be adopted again to carry out a compared analysis between two methods. PLAXIS 2D includes the functions that adopting SSR-FEM to calculated the safety factors and assuming shear strength linearly increasing with depth. Therefore, we can make a comparison of safety factors calculated by multi-block method and SSR-FEM. Because of the assumption that the support system is rigid, the corresponding model in the FEM should satisfy assumption. The meaning of rigid support systems includes two parts: firstly, the elastic limit of support systems is infinity; secondly, the support systems have enough rigidity so that the deformations can be ignored. In addition to the parameters in table 2, it is necessary to provide other key parameters for structure and soil in FEM model. Based on the previous study (Cheng 2019), the elastic model was adopted to simulate structure elements. The compressive stiffness (*EA*) of horizontal struts was $2.08 \times 10^4\ kN \cdot m$, and the two horizontal struts were set at -4m and -8m, respectively. The compressive stiffness (*EA*) and bending stiffness (*EI*) of support wall were $2.52 \times 10^7\ kN/m$ and $3.64 \times 10^6\ kN \cdot m^2/m$ (stiffness of per unit height), respectively. For soft clay, the elastic modulus adopted general empirical formula ($E_u = 250S_u = 8750\ kPa$), the Poisson's ratio was 0.3. The calculation results were shown in Fig. 6.

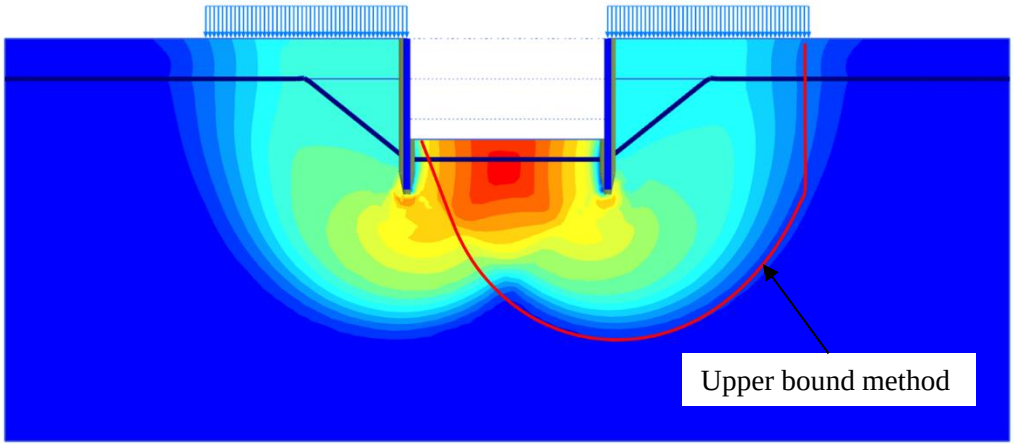

Fig. 6 the failure surfaces calculated by SSR-FEM and multi- block method.

In Fig. 6, the red curve was the failure surface calculated by multi-block method and the background figure is the incremental displacement cloud chart calculated by PLXIS 2D. Two failure surfaces almost coincide. And the safety factor of SSR-FEM is 2.862, the safety factor of multi-block method is 2.677. The relative error is 0.185 (about 6.9%). It is verified that the multi-block method is successfully applied to analyze the basal stability of braced excavation.

4. Case study

The excavation in Hangzhou is rectangle (190m×200m). The failure of support systems only occurs at the east wall in the mid of total project (Ying 2016). Therefore, the spatial effect of excavation can be ignored, and it can be analyzed as a plane strain problem. The soil above -30m is soft clay, and the soil below -30m is hard clay. Based on the assumption that failure surfaces would not cross hard layer, the search boundary in vertical direction was set -30m. The detail introduction is shown in Fig. 8. From Eq. (4), Eq. (6) and Eq. (8), it is ensured that $S_u(\xi, z) = (1.0488z + 14.89) \cdot [0.755 + 0.49\cos(2\xi + \pi/3)]$

It is worth noting that the support system is bored piles rather than diaphragm wall. Although the length of piles is 10.35 m longer than excavation depth, the toe of piles is not in hard layer. According to the report of accident, the cement mixing plies occurred serious deflections so that the excavation occurred basal heave failure. However, in the section 2.2, we assume that the support systems are rigid. In order to decrease the error between ideal model and project, the reduce factor ω is adopted. In this case, there are three results of calculation with $\omega = 0, 0.5, 1$, respectively. The detail results are shown in Table 3.

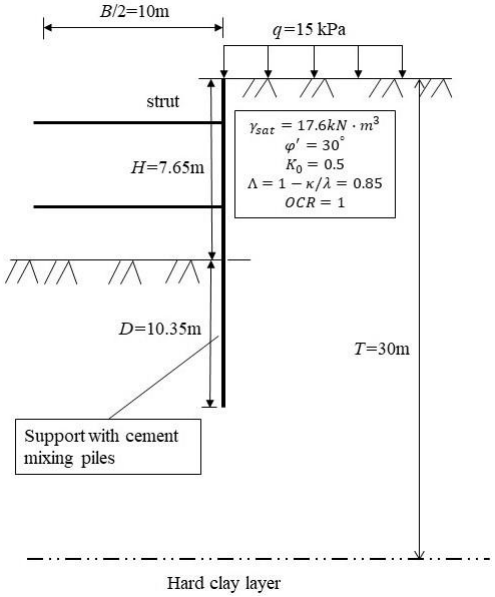

Fig. 8 The background of excavation in Hangzhou

Table 3 Calculation results of basal stability analysis for excavation in Hangzhou

Values of ω	Safety factor (F_S)			
	Calculation as isotropic soil ($k = 1$)		Calculation considering anisotropic soil ($k = 0.5$)	
	Results of Ying et al. (2016)	Results in this paper	Results of Ying et al. (2016)	Results in this paper
1	1.98	1.89	0.9	1.01
0.5	1.92	1.85	0.86	0.95
0	1.78	1.74	0.82	0.86

As shown in Table 3, the differences between considering anisotropy and isotropy are dramatic. The safety factor considering anisotropy is much lower than considering isotropy. In order to ensure the safety of engineering, it is necessary to consider anisotropy of soil. Besides, the influence of ω on safety factor is important, too. The reason is that the assumption that support systems are rigid is not always suitable for engineering, especially excavations which adopt cement mixing piles or bored piles to support and excavations in soft soil without an enough length of support wall. Actually, it is the serious deformations of support wall that lead to the basal heave failure. Therefore, in most cases, if this upper bound method is used to analysis the basal stability of excavations, the values of ω should be smaller than 1.

5. Conclusion

Based on the analysis, parameter studies and case studies, this paper applied the multi-block upper bound method to basal heave stability of braced excavations in anisotropic soft soils. Besides, the progressive search algorithm was adopted to improve the accuracy of calculating safety factor. Compared with traditional upper bound method, multi-block upper bound method only needed initial failure surfaces rather than detailed surfaces. And multi-block upper bound method could consider the

influence of parameters (factor of anisotropy, friction angle, depth-width ratio of excavation, length of support wall) on failure surfaces. The following conclusions can be drawn on the basis of the work presented herein:

(1) The number of failure surfaces ranges from 40 to 50, the initial length of search can be *B*/1000. For excavation whose size ranges from 20 to 40m, three phrases of search are suitable, four phrases will take more cost of calculations.

(2) In practical engineering, the factor of anisotropy plays a main role in basal heave stability of braced excavation. And for support wall consisting of cement mixing piles or bored piles, especially the toe of support wall above hard soil layer, the reduction factor should be lower than 0.5.

REFERENCES

Afiri, R. and Gabi, S. (2017), "Finite element slope stability analysis of Souk Tleta dam by shear strength reduction technique", *Innovative Infrastructure Solutions*, **3**(1),6.

Cai, L., Zhou, J., Ying, H.W. and Gong, X.N. (2018), "Stability against basal heave of excavation in anisotropic soft clay", *Chinese Journal of Geotechnical Engineering*, **40**(11),1968-1976. (in Chinese)

Casagrande, A., Carrillon, N. (1944), "Shear failure of anisotropic soil", *Journal of the Boston Society of Civil Engineers*, **31**(4),74-87.

Chang, M.F. (2000), "Basal Stability Analysis of Braced Cuts in Clay", Journal of Geotechnical and Geoenvironmental Engineering, **126**(3),276-279.

Chang, M.F., Teh, C.I. and Cao L. (1999), "Critical state strength parameters of saturated clays from the modified Cam clay model", *Canadian Geotechnical Journal*, **36**(5),876-890.

CHEN W.F. Limit analysis and soil plasticity. Amsterdam: Elsevier, 1975.

Chen, F.Y., Wang, L. and Zhang, W.G. (2019), "Reliability assessment on stability of tunnelling perpendicularly beneath an existing tunnel considering spatial variabilities of rock mass properties", *Tunnel Underground Space Technology*, **88**,276-289.

Chen, R.P., Li, Z.C., Chen, Y.M., Ou, C.Y., Hu, Q. and Rao, M. (2015), "Failure Investigation at a Collapsed Deep Excavation in Very Sensitive Organic Soft Clay", *Journal of Performance of Constructed Facilities*, **29**(3), 04014078.

Cheng, X.S., Li, X.H., Pan, J. and Zhen, G. (2019), "Basal-Heave Stability Analysis of Excavations Considering the Strength Reduction of Retaining Structures", *Journal of Tianjin University (Science and Technology)*, **52**(S1),56-62. (in Chinese)

Drucker, D.C., Prager, W. and Greenberg, H.J. (1952), "Extended Limit Design Theorems for Continuous Media", *Quarterly of Applied Mathematics*, **9**(4),381-389.

Faheem, H., Cai, F., Ugai, K. and Hagiwara, T. (2003), "Two-dimensional base stability of excavations in soft soils using FEM", *Computers and Geotechnics*, **30**(2),141-163.

Gao, Y.F., Ye, M. and Zhang, F. (2015), "Three-dimensional analysis of slopes reinforced with piles", *Journal of Central South University*, **22**(6),2322-2327.

Goh, A.T.C. (1994), "Estimating basal-heave stability for braced excavations in soft clay", *Journal of Geotechnical Engineering, ASCE*, **120**(8),1430-1436.

Goh, A.T.C. (2017a), "Deterministic and reliability assessment of basal heave stability for braced excavations with jet grout base slab", *Engineering Geology*, **218**:63-69.

Goh, A.T.C. (2017b), “Basal heave stability of supported circular excavations in clay”, *Tunnel and Underground Space Technology*, **61**,145-149.

Goh, A.T.C., Kulhawy, F.H. and Wong, K.S. (2008), “Reliability assessment of basal-heave stability for braced excavations in clay”, *Journal of Geotechnical and Geoenvironmental Engineering*, **134**(2),145-153.

Greco, V.R. (1996), “Efficient Monte Carlo technique for locating critical slip surface”, *Journal of Geotechnical Engineering, ASCE*, **122**(7),517-525.

Han, C.Y., Chen, J.J., Xia, X.H. and Wang, J.H. (2014), “Three-dimensional stability analysis of anisotropic and non-homogeneous slopes using limit analysis”, *Journal of Central South University*, **21**(3),1142-1147.

Huang, M.S. and Qin, H.L. (2009), “Upper-bound multi-rigid-block solutions for bearing capacity of two-layered soils”, *Computers and Geotechnics*, **36**(3),525-529.

Huang, M.S., Tang, Z. and Yuan, J.Y. (2018), “Basal stability analysis of braced excavations with embedded walls in undrained clay using the upper bound theorem”, *Tunnel and Underground Space Technology*, **79**,231-241.

Luo, Z., Di, H.G., Kamalzare, M. and Li, Y.X. (2020), “Effects of soil spatial variability on structural reliability assessment in excavations”, *Underground Space*, **5**(1),71-83.

Malkawi, A.I.H., Hassan, W.F. and Sarma, S.K. (2001b), “An efficient search method for finding the critical circular slip surface using the Monte Carlo technique”, *Canadian Geotechnical Journal*, **38**(5),1081-1089.

Malkawi, A.I.H., Hassan, W.F., Sarma, S.K. (2001a), “Global search method for locating general slip surface using Monte Carlo techniques”, *Journal of Geotechnical and Geoenvironmental Engineering*, **127**(8),688-698.

Michalowski, R.L. and Drescher, A. (2009), “Three-dimensional stability of slopes and excavations”, *Geotechnique*, **59**(10),839-850.

Mroz, Z., Norris, V.A. and Zienkiewicz, O.C. (1978), “Anisotropic Hardening Model for Soils and Its Application to Cyclic Loading”, *International Journal for Numerical and Analytical Methods in Geomechanics*, **2**(3),203-221.

Mroz, Z., Norris, V.A., Zienkiewicz, O.C. (1979), “Application of an Anisotropic Hardening Model in the Analysis of Elastoplastic Deformation of Soils”, *Geotechnique*, **29**(1),1-34.

Otha, H. and Nishihara, A. (1985), “Anisotropy of undrained shear strength of clays under axi-symmetric loading conditions”, *Soils and Foundations*, **25**(2),73-86.

Qin, H.L., Chen, Z.Y. and Liu, L.P. (2012), “Basal stability analysis for excavations in soft clay based on upper bound method”, *Chinese Journal of Geotechnical Engineering*, **34**(9),1611-1619. (in Chinese)

Qin, H.L., Huang, M.S. and Ma, S.K. (2010a), “Multi-block upper bound method for basal heave stability analysis of braced excavations in clay”, *Chinese Journal of Rock Mechanics and Engineering*, **29**(1),73-81. (in Chinese)

Qin, H.L., Huang, M.S. and Wang, Y.J. (2010b), “Application of Monte Carlo search technique to bearing capacity calculations by upper bound method”, *Rock and Soil Mechanics*, **31**(10),3145-3150. (in Chinese)

Shen, K.L. Degradation of soil structure and plasticity evolution of natural clay: Zhejiang University, 2006. (in Chinese)

Su, S.F., Liao, H.J. and Lin, Y.H. (1998), "Base stability of deep excavation in anisotropic soft clay", *Journal of Geotechnical and Geoenvironmental Engineering*, **124**(9),809-819.

Ukritchon B., Whittle, A.J. and Sloan, S.W. (2003), "Undrained stability of braced excavations in clay", *Journal of Geotechnical and Geoenvironmental Engineering*, **129** (8):738-755.

Ukritchon, B., Yingchaloenkitkhajorn, K. and Keawsawasvong, S. (2017), "Three-dimensional undrained tunnel face stability in clay with a linearly increasing shear strength with depth". *Computers and Geotechnics*, **88**,146-151.

Wang, L. and Long, F. (2014), "Base stability analysis of braced deep excavation in undrained anisotropic clay with upper bound theory", *Science China-Technological Sciences*, **57**(9),1865-1876.

Yang, X.L. and Du, D.C. (2016), "Upper bound analysis for bearing capacity of nonhomogeneous and anisotropic clay foundation", *Journal of Civil Engineering*, *KSCE*, **20**(7),2702-2710.

Ying, H.W., Zhang, J.H., Zhou, J., Sun, W. and Yan, J.J. (2016), "Analysis of stability against basal heave of excavation in anisotropic soft clay based on tests of hollow cylinder apparatus". *Rock and Soil Mechanics*, **37**(5),1237-1242. (in Chinese)

Zou, G.D. (2004), "Analysis of stability against upheaval of deep excavation by an upper limit method", *Rock and Soil Mechanics*, **25**(12),1873-1878. (in Chinese)